Isentropic compression of hydrogen: Probing conditions deep in planetary interiors

Andreas Becker,[1] Nadine Nettelmann,[2] Bastian Holst,[3] and Ronald Redmer[1]
[1]*Institut für Physik, Universität Rostock, D-18051 Rostock, Germany*
[2]*Department of Astronomy and Astrophysics, University of California, Santa Cruz, California 95064, USA*
[3]*CEA, DAM, DIF, F-91297 Arpajon, France*
(Received 28 November 2012; revised manuscript received 8 March 2013; published 19 July 2013)

We perform *ab initio* calculations for the equation of state of dense liquid hydrogen and deuterium using quantum molecular dynamics simulations based on finite-temperature density functional theory. This extensive data set allows us to determine specific density-temperature-pressure tracks such as the cold curve, precompressed and principal Hugoniot curves, and isentropes which are essential for the analysis and interpretation of high-pressure experiments. In this study we focus on conditions probed by recent quasi-isentropic shock compression experiments that have reached a so-far unprecedented 108-fold compression of gaseous deuterium. As these states of matter are relevant for the deep interior of Jupiter-like exoplanets we simultaneously give predictions for their isentropes.

DOI: 10.1103/PhysRevB.88.045122 PACS number(s): 62.50.−p, 64.30.−t, 96.15.Nd, 52.65.Yy

I. INTRODUCTION

The equation of state (EOS) of dense hydrogen is of fundamental interest because of wide applications in astrophysics, for instance for interior models of solar and extrasolar giant planets.[1–4] Furthermore, important features of the high-pressure phase diagram of this simplest element, e.g., the slope of the melting line, the transition pressure to solid metallic hydrogen, and the location of a first-order liquid-liquid transition between a metallic and a nonmetallic phase with a second critical point above 1 Mbar and below 2000 K, are still poorly known; for a recent review, see Ref. 5.

To probe matter under such extreme conditions is a challenging task. Dynamical methods using high-power lasers, gas guns, pulsed power, and chemical explosions as drivers for strong shock waves were implemented for this purpose. The pressure-temperature region probed by single shock experiments is fixed by the Hugoniot curve with a maximum compression of about 4.25–4.50 (Refs. 6–9) for an initial state of cryogenic liquid hydrogen at 20 K and 0.071 g/cm^3 (or liquid deuterium at 20 K and 0.172 g/cm^3). States off the principal Hugoniot curve can be investigated by varying the initial conditions via solid or gaseous targets,[10,11] applying reverberating shock waves,[7,8,12] or using isentropic compression that generates high pressures at moderate temperatures.[13–15]

Isentropic compression also probes conditions along a planetary isentrope if the initial conditions are chosen appropriately. This would allow us to discriminate between competing planetary interior models. For instance, even for Jupiter, the size of the core and the distribution of heavier elements (other than H and He) throughout the planet are still under debate.[16]

The aim of the present paper is to compare our *ab initio* EOS data with results of recent high-pressure experiments. Of particular interest are experiments with quasi-isentropic compression paths that probe so-far unprecedented states of matter. Furthermore, we calculate isentropes through Jupiter-like exoplanets.

We perform molecular dynamics simulations based on finite-temperature density functional theory (DFT-MD) and calculate the isentropes along the experimental paths. We characterize the predicted thermodynamic states and analyze whether or not quasi-isentropic compression has been achieved in these setups. This paper is arranged as follows. We give details of our EOS simulations and determination of isentropes in Sec. II and show extensive calculations and comparisons with high-pressure experiments, especially isentropic compression experiments, in Sec. III. The conclusions are drawn in Sec. IV.

II. *AB INITIO* HYDROGEN EOS

The DFT-MD framework combines classical molecular dynamics simulations for the ions with a quantum treatment for the electrons based on DFT,[17] which is implemented in the VASP program package.[18–20] The Coulomb interactions between the electrons and ions are treated using projector-augmented wave potentials[21,22] at densities below 9 g/cm^3 with a converged energy cutoff of 1200 eV. In particular, for densities above 1 g/cm^3 we apply the hard potential provided by VASP with a cutoff radius of 0.43 Å, while for lower densities we apply the soft potential with a cutoff radius of 0.52 Å.

The forces that act on the ions are derived via the Hellmann-Feynman theorem at each MD step. This procedure is repeatedly performed in a cubic simulation box with periodic boundary conditions for several thousand MD steps of 0.1–1 fs duration so that the total simulation time amounts up to 10 ps. The ion temperature is controlled with a Nosé thermostat.[23]

Convergence is checked with respect to the particle number, the **k**-point sets used for the evaluation of the Brillouin zone, and the energy cutoff for the plane-wave basis set. For the simulations we chose 256 atoms and the Baldereschi mean value point[24] which proved to yield well converged simulation runs.[25,26]

We use the exchange-correlation functional of Perdew, Burke, and Ernzerhof (PBE),[27] which has been shown to give reasonable results for warm dense matter states.[25,26] Zero-point motion (ZPM) of the ions bound in molecules are treated as follows. The fraction of molecules in the box (α_m) is determined via the coordination number; see Ref. 25. Then, the quantum-mechanical correction to the internal energy per particle with respect to molecular vibrations (ΔU) is

performed according to Ref. 28 by subtracting the classical vibrational energy and adding the contribution of the quantum-mechanical harmonic oscillator via

$$\Delta U = \alpha_m \frac{1}{2} k_B \left[\Theta_{\rm vib} \left(\frac{1}{2} + \frac{1}{\exp(\Theta_{\rm vib}/T) - 1} \right) - T \right], \quad (1)$$

where k_B is the Boltzmann constant and T is the temperature of the system. The vibrational temperatures $\Theta_{\rm vib}^{H_2} = 6338.2$ K and $\Theta_{\rm vib}^{D_2} = 4482$ K are taken from Ref. 29. While this approach is suitable to treat molecules it fails in estimating ZPM effects for the protons, which are not considered in our EOS data. Quantum Monte Carlo calculations, as performed by Morales *et al.*,[30] are able to predict the effects of protonic ZPM. Based on their results we estimate an error of maximal 1% for our thermal and 0.5% for our caloric EOS in the partly dissociated and atomic regime.

Our present hydrogen EOS table used within this paper contains 20 isotherms between 60 and 50 000 K and 21 isochores between 0.07 and 9 g/cm^3. It is a substantial extension of the EOS data set reported recently in Ref. 4. To describe experiments performed with deuterium, we scale the hydrogen EOS by a factor of 2 in density but account for the correct starting point of the Hugoniot curve ($T = 20$ K, $\rho = 0.172$ g/cm^3) which is calculated with DFT-MD runs as well; see Ref. 31. Some experiments start at initial conditions below 0.1 g/cm^3. For these low densities we include data of Leachman[32] ($T \leqslant 1000$ K) and data derived within fluid variational theory[33] ($T > 1000$ K) in our EOS table. Several EOS data for hydrogen derived from first-principles methods were proposed, e.g., by Caillabet *et al.*[34] using DFT-MD and by Morales *et al.*[30] using a coupled electron-ion Monte Carlo (CEIMC) method. Our data are in a very good agreement with their results; see Fig. 1. Solid lines represent our DFT-MD EOS, and squares and triangles represent those of Refs. 30 and 34. The coincidence of the 300 and 1000 K isotherme around 1 g/cm^3 is caused by the first-order liquid-liquid phase transition in that region; see Refs. 26 and 36.

Finally, we calculate isentropes for given initial temperatures and densities according to the following first-order differential equation:

$$\left(\frac{\partial T}{\partial \rho} \right)_S = \frac{T}{\rho^2} \frac{\left(\frac{\partial P}{\partial T} \right)_\rho}{\left(\frac{\partial u}{\partial T} \right)_\rho} \quad . \quad (2)$$

Equation (2) states that the slope of the temperature T with respect to the density ρ at constant entropy S is given by the absolute values of T and ρ together with the change of the pressure P and specific internal energy $u = U/m$ with temperature at constant density. Arbitrary EOS points between our DFT-MD grid, required for the discretization of the densities, are generated via cubic spline interpolation.

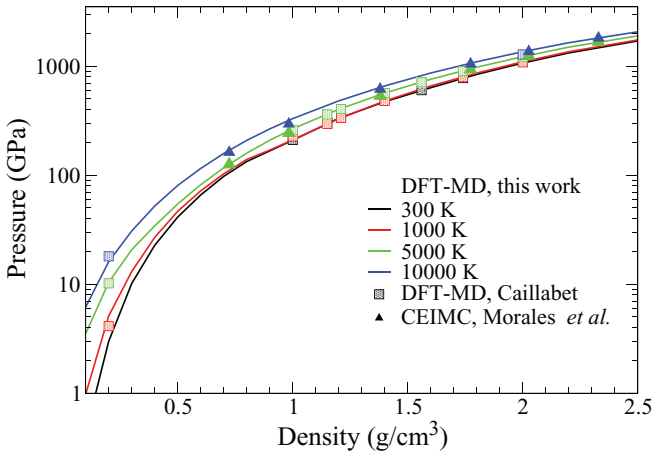

FIG. 1. (Color online) Our DFT-MD isotherms (solid lines) of 300 K (black), 1000 K (red), 5000 K (green), 10 000 K (blue) in comparison with CEIMC data from Morales *et al.* (Ref. 30) (triangles) and Caillabet (Ref. 35) (squares).

III. HIGH-PRESSURE EXPERIMENTS

Several experiments, especially to probe the off-Hugoniot states of the EOS, have been performed recently. In this section we reconstruct those experiments using our EOS focusing on quasi-isentropic shocks.

A. Hugoniot curves

High pressures are generated in single shock experiments. With known initial conditions and measured shock wave and pusher velocities, pressure and density are determined via the Hugoniot equations so that a $P(\rho)$ relation is derived. Additional measurement of the temperature would lead to the thermal EOS $P(\rho,T)$; see Ref. 9. We will focus here on results obtained with the Z machine[7,8] for the principal Hugoniot of deuterium shown in Fig. 2. This data set is in very good agreement with earlier *ab initio* simulations[25,37] and our DFT-MD data. In addition, we have calculated second shock Hugoniot curves starting at 1000 K and 0.434 g/cm^3 and 10 000 K and 0.757 g/cm^3 and compare these with the respective isentropes. For 1000 K both curves have the same slope up to 1.2 g/cm^3 and for 10 000 K up to 1.0 g/cm^3, i.e., the lower the initial temperature of the second shock the

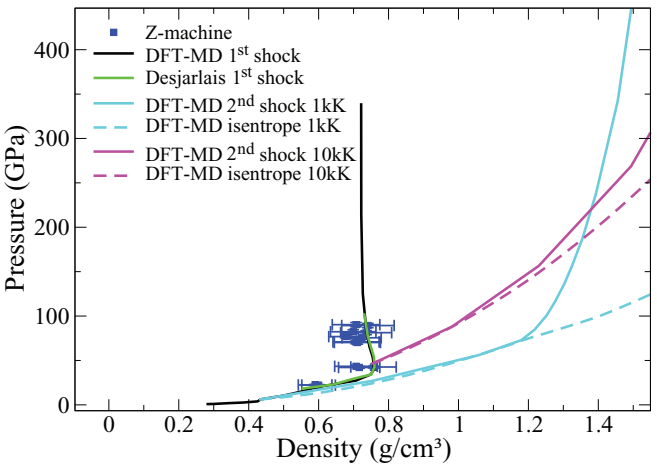

FIG. 2. (Color online) Hugoniot curves for deuterium. Experiments: Z machine (blue squares) (Refs. 7 and 8). DFT-MD: Desjarlais (green solid) (Ref. 37); present results (black solid). Also shown are second shock Hugoniot curves (solid) and respective isentropes (dashed) starting from 1000 K and 0.434 g/cm^3 (cyan) and from 10 000 K and 0.757 g/cm^3 (magenta).

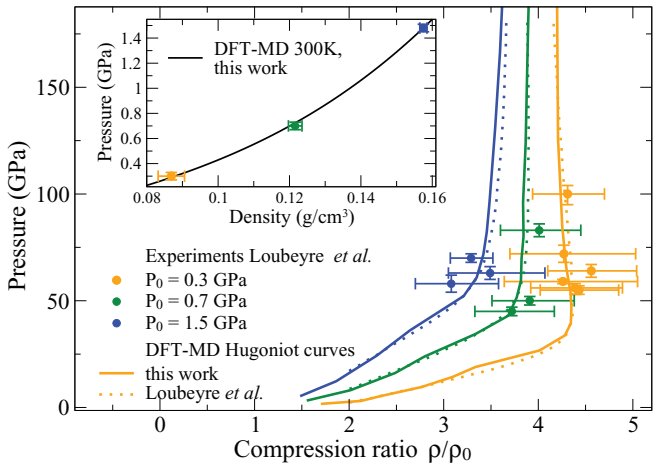

FIG. 3. (Color online) Hugoniot curves generated from precompressed hydrogen ($T = 297$ K) with initial pressures of 0.3 GPa (orange), 0.7 GPa (green), and 1.6 GPa (blue), respectively. Experimental points and theoretical DFT-MD curves (dashed) of Loubeyre *et al*. (Ref. 11) are compared with our results (solid). Inset: Initial precompressed states of Ref. 11 (same color code as in main frame) coincide with our 300 K DFT-MD isotherm (black solid).

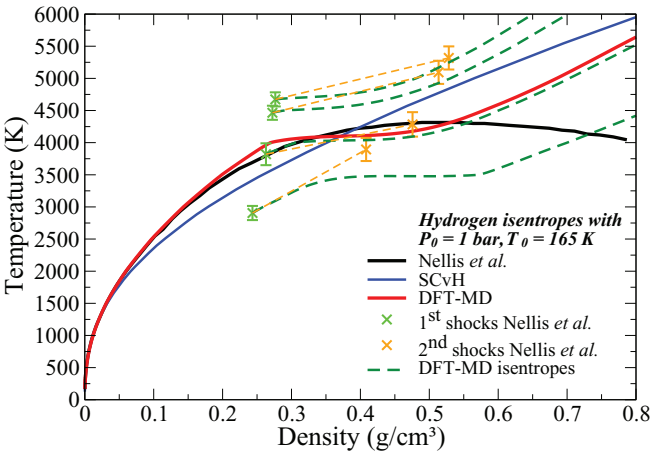

FIG. 4. (Color online) Reverberating shock wave experiments for hydrogen (Ref. 39) (crosses), first shock (green), and second shock data (orange), each pair connected by a dashed orange line. The DFT-MD isentropes (dashed green) start from the first shocks. The hydrogen isentropes for Jovian conditions were calculated by Nellis *et al*. (Ref. 39) (black), SCvH (Ref. 41) (blue), and with the present DFT-MD data (red).

more isentropic the compression becomes. Similar results have recently been found for water.[38]

Off-hugoniot states of hydrogen and deuterium were also measured by laser-shocking an isothermally precompressed sample in a diamond-anvil cell by Loubeyre *et al*.[11] They generated initial pressures of 0.16, 0.3, 0.7, and 1.6 GPa with an initial temperature of 297 K and reached final shocked states up to 175 GPa. Results are compared in their paper with theoretical predictions from the DFT-MD EOS of Caillabet *et al*.[34] We calculate corresponding precompressed Hugoniots curves for hydrogen using our EOS starting from 300 K with the respective pressures. They match the experimental data very well; see inset of Fig. 3. The results shown in the main frame of Fig. 3 illustrate the remarkable coincidence of both *ab initio* Hugoniot curves with each other and with the experimental points. Furthermore, we agree perfectly with the theoretical temperature-pressure curves in Fig. 6 in Ref. 11. Notice that both theoretical curves are slightly lower than the experimental temperatures. This difference may originate from the use of the PBE exchange-correlation functional that underestimates the band gap, yielding to an onset of metallization at slightly lower temperatures.

B. Reverberating shocks

The reverberating shock wave experiments for hydrogen reported by Nellis and co-workers[39,40] probed temperatures and densities relevant for the interior of Jupiter; see Fig. 4. Based on these data, an EOS was constructed in order to calculate a hydrogen isentrope for Jovian conditions, starting at a surface temperature of 165 K at 1 bar. For comparison we show associated isentropes calculated with the EOS of Saumon *et al*. (SCvH)[41] and our DFT-MD results. In contrast to the SCvH isentrope, the experimental and the DFT-MD isentropes flatten in slope at about 0.3 g/cm^3 which is due to dissociation of hydrogen molecules; see Refs. 39 and 42. The saddle point of the flattening is situated at slightly lower conditions at the DFT-MD isentrope, again because of the band-gap problem mentioned above. For higher temperatures and densities hydrogen is completely dissociated and our DFT-MD data yield another increase. This is in contrast to the slope of the isentrope of Nellis *et al*., who extrapolated their data beyond 0.52 g/cm^3. However, it should be remembered that in the density-temperature range where experimental data are available the DFT-MD isentrope and the experimental one coincide.

In addition, we predict possible second shock states by calculating DFT-MD isentropes starting from the first shocks; see Fig. 4. These curves reproduce correctly three second shock data which support the assumption that the reflected shock is isentropic; see Fig. 2. The slight discrepancy for the lowest data point could result from the band-gap problem mentioned in Sec. III A that predicts dissociation, and by association the flattening of the isentrope, at slightly lower temperatures.

C. Quasi-isentropic compression

Quasi-isentropic shock wave experiments using high explosives were performed recently to study the nonmetal-to-metal transition in hydrogen and deuterium,[13] the behavior of hydrogen at pressures up to about 18 Mbar,[14] and the high-pressure cold curve of hydrogen and deuterium.[15] The sample in each experiment was compressed by high explosives using cylindrical or spherical symmetry. X-ray backlighting yielded the compression ratio and hence the density. Associated temperatures were estimated *a postiori* by hydrodynamic simulations that reproduced the measured compression ratios. These simulations used the existing model EOS, in particular those given in Refs. 43 and 44. Determinations of the pressures differ within the experiments and will be discussed separately below.

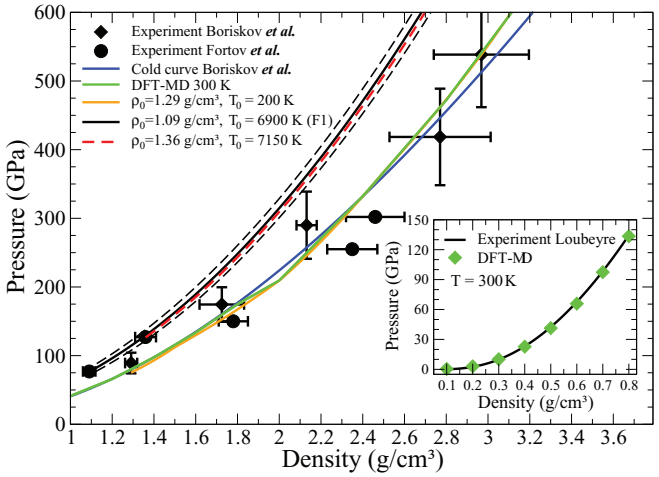

FIG. 5. (Color online) Quasi-isentropic compression experiments of Boriskov *et al*. (Ref. 15) (diamonds) and Fortov *et al*. (Ref. 13) (circles) for deuterium. DFT-MD isentropes start from the first point of Boriskov *et al*. (orange), and from the first (black, labeled F1) and second (red) experimental point of Fortov *et al*. The respective cold curve of Boriskov *et al*. (blue) and the 300 K DFT-MD isotherm (green) are also shown. Inset: 300 K isotherm (cold curve) for hydrogen from diamond-anvil cell experiments of Loubeyre *et al*. (Ref. 45) (black line) compared with DFT-MD data (red diamonds).

In the following we compare each quasi-isentropic experiment with results from our DFT-MD EOS. We calculate DFT-MD isentropes for given initial temperatures T_0 and densities ρ_0 using Eq. (2).

The first item is the experimental investigation of the high-pressure cold curve of hydrogen and deuterium. Static measurement at room temperature on that issue has been performed by Loubeyre *et al*.[45] Our DFT-MD 300 K isotherm for hydrogen is in excellent agreement with their data; see the inset of Fig. 5.

However, a dynamic approach was chosen within the quasi-isentropic experiment of Boriskov *et al*.[15] They measured the density and simultaneously the pressure $P(\rho)$ of the system via an aluminum layer in the vicinity of the sample using the experimental reference data reported in Ref. 46.

Since our DFT-MD data do not cover their initial temperature of ∼10 K we calculate an isentrope for deuterium starting from their first data point, i.e., $T_0 = 200$ K, $\rho_0 = 1.29$ g/cm^3, and $P_0 = 75$ GPa. We find a very good agreement with their data within the error bars; see Fig. 5. Our isentrope (orange) agrees very well with our 300 K isotherm (green) and their high-pressure cold curve (blue). Based on this result we can confirm their calculated temperatures, as well, that remain at about 300 K; see Table I.

Within another quasi-isentropic experiment Fortov *et al*.[13] found first signatures of a first-order phase transition due to the nonmetal-to-metal transition [plasma phase transition (PPT)] in dense deuterium. They started from a gaseous initial state of $\rho_0 = 0.04$ g/cm^3 and $T_0 = 283$ K. In contrast to the experiment of Boriskov *et al*. they only measured the densities. The pressures were determined afterwards using a hydrocode with model EOS,[43,44] similar to the temperature calculations described above. Their results are plotted as circles in Fig. 5.

TABLE I. Predictions of pressures and temperatures for isentropic compression experiments for deuterium based on DFT-MD simulations. The calculated values from the corresponding experimental papers are given in parentheses below our results. Notice that Fortov *et al*. (Ref. 13) used two model EOS.

Data point	Fortov *et al*. (Ref. 13) ρ (g/cm^3)	T (K)	P (GPa)
1	1.09	890	55
		(3100, 2180)	(77)
2	1.36	950	91
		(3850, 2500)	(127)
3	1.78	1030	164
		(4100, 2600)	(150)
4	2.35	1140	315
		(5200, . . .)	(255)
5	2.46	1160	352
		(. . . , 2410)	(302)
	Mochalov *et al*. (Ref. 14)		
1	4.3	1470	1300
		(3500)	(1800)
	Boriskov *et al*. (Ref. 15)		
1	1.29	200	75
		(<300)	(89)
2	1.73	280	154
		(<300)	(175)
3	2.13	295	245
		(<300)	(290)
4	2.77	330	461
		(<300)	(420)
5	2.97	335	536
		(<300)	(540)

They conclude the signature of the PPT from the density jump indicated by the third data point. A proper theoretical confirmation of this feature is an outstanding problem since numerous and different predictions for the PPT have been given in the past, mostly based on chemical models. Recent first-principles simulations[26,36] have predicted the PPT in the dense liquid with a critical point below $T_c \sim 2000$ K and above $P_c \sim 100$ GPa. Inclusion of nuclear quantum effects, a nonlocal exchange-correlation functional and of van der Waals corrections may shift the transition considerably; see Ref. 47.

However, these critical parameters are well below the results of Fortov *et al*. Therefore we expect for those pressure-temperature data a continuous transition from the nonmetallic molecular to the metallic atomic phase in that supercritical region, which is accompanied by a sharp but smooth increase of the electrical conductivity. This behavior was found in the experiments; see Ref. 13.

For fixed initial conditions all measured points of a quasi-isentropic compression experiment have to be located along an isentrope. As mentioned above, pressures and temperatures with respect to the measured densities rely on model EOS. These data deviate significantly from our DFT-MD data. For instance, for a density of 1.09 g/cm^3 and a pressure of 77 GPa we obtain a temperature of 6900 K from our EOS instead of the 3100 or 2100 K given in Ref. 13. Using this point

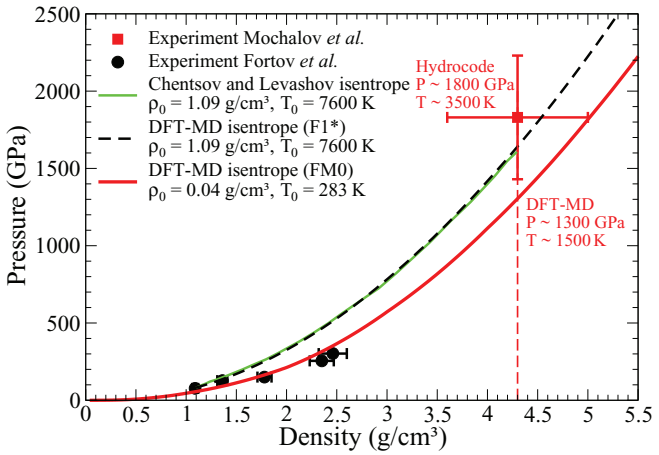

FIG. 6. (Color online) Quasi-isentropic compression experiments of Mochalov *et al*. (Ref. 14) (square) and Fortov *et al*. (Ref. 13) (circles) are compared with the DFT-MD isentrope starting from the same gaseous initial condition (red solid, labeled FM0). Also shown are isentropes starting from the first point of Ref. 13 calculated by Chentsov and Levashov (Ref. 48) (green solid), which agree with our DFT-MD curve (black dashed, labeled F1*).

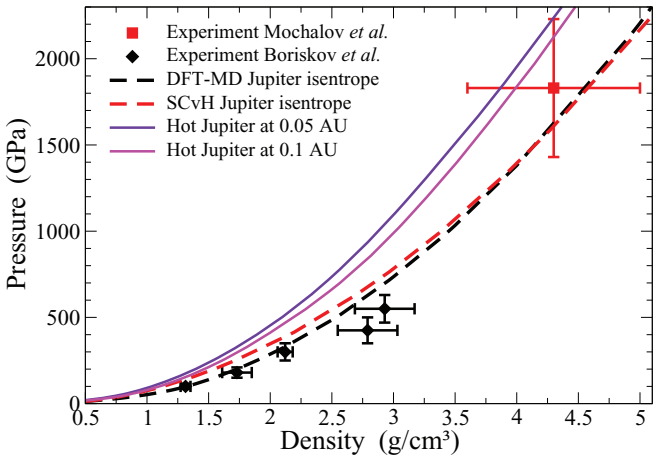

FIG. 7. (Color online) H-He isentropes for Jupiter conditions calculated with DFT-MD data (black dashed) and the SCvH-EOS (Ref. 41) (red dashed), isentropes of Jupiter-mass exoplanets, and experimental data for deuterium. Exoplanets at 0.1 astronomical unit (AU) distance from its host star with $T(100\,\text{bars}) = 1625$ K (magenta) and at 0.05 AU with $T(100\,\text{bars}) = 1320$ K (violet).

($\rho_0 = 1.09$ g/cm^3, $T_0 = 6900$ K) as the initial condition for a further isentropic compression, the resulting track (hereafter F1: black solid line in Fig. 5, and dashed lines for the experimental error bars of the density) reproduces only the second data point well and the respective isentrope calculated from there (red dashed line in Fig. 5). Although all points should be located on the same isentrope, both isentropes are well above the remaining three points while the two highest compressions are even below the experimental and DFT-MD high-pressure cold curves; see Fig. 5. In particular the temperatures and pressures at these points appear to be questionable.

Similar *ab initio* simulations have been performed in this context[48] which start from the given density and pressure of the first data point with a temperature of 7600 K, higher than our result (6900 K; see Fig. 5). We confirm their isentrope with this initial condition; see green solid line in Fig. 6 (hereafter F1*).

While the isentropes using the first data point as initial conditions (F1 and F1*) depend on the calculated pressure of 77 GPa, we construct another one using the theory-independent initial conditions of this experiment, namely gaseous deuterium at $\rho_0 = 0.04$ g/cm^3 and $T_0 = 283$ K. The resulting isentrope (hereafter FM0) that reconstructs the full experimental path is shown as the red solid curve in Fig. 6. Interestingly, FM0 proceeds smoothly but with a significant deviation between the data of Fortov *et al*. The associated numerical values are presented in Table I.

An extension of the experiment of Fortov *et al*. towards a much higher compression ratio of $\rho/\rho_0 \sim 108$ has been performed by Mochalov *et al*.[14] They started from the same gaseous initial state of deuterium as in Ref. 13. Based on hydrodynamic simulations and the model EOS of Ref. 43, they predicted a so-far unprecedented pressure for D_2 of 18 Mbar and a temperature of 3500 K at the measured density of 4.3 g/cm^3. From our FM0 (red solid curve in Fig. 6) we predict a significantly lower pressure of ∼13 Mbar and a temperature of 1500 K at the measured density for this experiment; see Table I. As shown in Fig. 6, our FM0 connects the experiment of Mochalov *et al*. and the one of Fortov *et al*. with respect to all data points. Actually this track reconstructs these experiments better than the isentrope starting from the first data point of Fortov *et al*. (F1 and F1*), where only three data points out of six are located on that isentrope.

D. Isentropes of Jupiter-mass exoplanets

Particularly noteworthy in this context is that high pressures as relevant for the deep interior of giant planets can now be probed in laboratory experiments. Accurate results, e.g., a fully measured $P(\rho, T)$, would help to discriminate between competing interior models.[16] As a first example of possible compression pathways, we compare isentropes through Jupiter and some Jupiter-like exoplanets in Fig. 7. Displayed is the partial hydrogen density of computed H-He isentropes with solar H-He mass ratio, scaled by a factor of 2 in density. The Jupiter isentrope is defined by the outer boundary condition $T(1\,\text{bar}) = 170$ K for which we compare our DFT-MD isentrope with that derived from SCvH.[41] The hot Jupiter isentropes are defined by the outer boundary conditions at the 100-bar level for Jupiter-mass exoplanets after 4.5 Gyr of cooling according to Fig. 3 in Ref. 49. The isentropes in Fig. 7 may serve to design new quasi-isentropic experiments by providing possible initial conditions and predicting theoretical compression pathways.

IV. CONCLUSIONS

We performed DFT-MD simulations for a wide range of parameters and constructed a hydrogen EOS which reproduces principal and precompressed Hugoniot curves and diamond-anvil cell experiments very well and coincide with other first-principles EOS data.[30,34] We find that second shock Hugoniot curves follow isentropes with the same initial conditions for a long segment of the density-pressure plane. Furthermore,

a very good agreement of our hydrogen isentrope for Jovian conditions with that of Nellis *et al.*[39] based on experimental data can be stated.

Our DFT-MD results agree very well with the quasi-isentropic compression experiment of Boriskov *et al.*[15] On the contrary, we cannot confirm those data of Fortov *et al.*[13] that are located below the experimental and our theoretical cold curve. In particular, we find no signatures of a phase transition in the range of their predicted pressure-temperature data points. However, we find a pathway for the isentropic compression of gaseous deuterium (FM0) which connects the Fortov *et al.* data and the high-pressure point of Mochalov *et al.*[14] using the initial condition of their experiments. Our DFT-MD predictions for the experimental point of Mochalov *et al.* are rather 13 Mbar than their estimated 18 Mbar that is based on a model EOS; see Table I. Isentropic compression experiments can probe conditions deep in the interior of Jupiter-like exoplanets. This would help to discriminate between current interior models if one succeeds to measure the pressure and temperature simultaneously with the density. We give exemplary isentropes through Jupiter-like exoplanets in order to design such challenging experiments.

ACKNOWLEDGMENTS

We thank W. Lorenzen, M. Bethkenhagen, M. French, M. P. Desjarlais, M. D. Knudson, V. K. Gryaznov, V. B. Mintsev, and V. E. Fortov for helpful discussions. This work was supported by the Deutsche Forschungsgemeinschaft within the SFB 652. The DFT-MD simulations were performed at the North-German Supercomputing Alliance (HLRN) and at the IT and Media Center of the University of Rostock.

[1] T. Guillot, Science **286**, 72 (1999).
[2] N. Nettelmann, B. Holst, A. Kietzmann, M. French, R. Redmer, and D. Blaschke, Astrophys. J. **683**, 1217 (2008).
[3] J. J. Fortney and N. Nettelmann, Space Sci. Rev. **152**, 423 (2010).
[4] N. Nettelmann, A. Becker, B. Holst, and R. Redmer, Astrophys. J. **750**, 52 (2012).
[5] J. M. McMahon, M. A. Morales, C. Pierleoni, and D. M. Ceperley, Rev. Mod. Phys. **84**, 1607 (2012).
[6] M. D. Knudson, D. L. Hanson, J. E. Bailey, C. A. Hall, J. R. Asay, and W. W. Anderson, Phys. Rev. Lett. **87**, 225501 (2001).
[7] M. D. Knudson, D. L. Hanson, J. E. Bailey, C. A. Hall, and J. R. Asay, Phys. Rev. Lett. **90**, 035505 (2003).
[8] M. D. Knudson, D. L. Hanson, J. E. Bailey, C. A. Hall, J. R. Asay, and C. Deeney, Phys. Rev. B **69**, 144209 (2004).
[9] T. Sano, N. Ozaki, T. Sakaiya, K. Shigemori, M. Ikoma, T. Kimura, K. Miyanishi, T. Endo, A. Shiroshita, H. Takahashi, T. Jitsui, Y. Hori, Y. Hironaka, A. Iwamoto, T. Kadono, M. Nakai, T. Okuchi, K. Otani, K. Shimizu, T. Kondo, R. Kodama, and K. Mima, Phys. Rev. B **83**, 054117 (2011).
[10] S. Grishechkin, S. Gruzdev, V. Gryaznov, M. Zhernokletov, R. Ilkaev, I. Iosilevskii, G. Kashintseva, S. Kirshanov, S. Manachkin, V. Mintsev *et al.*, JETP Lett. **80**, 398 (2004).
[11] P. Loubeyre, S. Brygoo, J. Eggert, P. M. Celliers, D. K. Spaulding, J. R. Rygg, T. R. Boehly, G. W. Collins, and R. Jeanloz, Phys. Rev. B **86**, 144115 (2012).
[12] S. T. Weir, A. C. Mitchell, and W. J. Nellis, Phys. Rev. Lett. **76**, 1860 (1996).
[13] V. E. Fortov, R. I. Ilkaev, V. A. Arinin, V. V. Burtzev, V. A. Golubev, I. L. Iosilevskiy, V. V. Khrustalev, A. L. Mikhailov, M. A. Mochalov, V. Y. Ternovoi, and M. V. Zhernokletov, Phys. Rev. Lett. **99**, 185001 (2007).
[14] M. A. Mochalov, R. I. Ilkaev, V. E. Fortov, A. L. Mikhailov, Y. M. Makarov, V. A. Arinin, S. K. Grishechkin, A. O. Blikov, V. A. Ogorodnikov, A. V. Ryzhkov, and V. K. Gryaznov, JETP Lett. **92**, 300 (2010).
[15] G. V. Boriskov, A. I. Bykov, N. I. Egorov, M. I. Dolotenko, V. N. Pavlov, and V. I. Timareva, Contrib. Plasma Phys. **51**, 339 (2011).
[16] N. Nettelmann, Adv. Space Sci. **336**, 47 (2011).
[17] N. D. Mermin, Phys. Rev. **137**, A1441 (1965).
[18] G. Kresse and J. Hafner, Phys. Rev. B **47**, 558 (1993).
[19] G. Kresse and J. Hafner, Phys. Rev. B **49**, 14251 (1994).
[20] G. Kresse and J. Furthmüller, Phys. Rev. B **54**, 11169 (1996).
[21] P. E. Blöchl, Phys. Rev. B **50**, 17953 (1994).
[22] G. Kresse and D. Joubert, Phys. Rev. B **59**, 1758 (1999).
[23] S. Nosé, J. Chem. Phys. **81**, 511 (1984).
[24] A. Baldereschi, Phys. Rev. B **7**, 5212 (1973).
[25] B. Holst, R. Redmer, and M. P. Desjarlais, Phys. Rev. B **77**, 184201 (2008).
[26] W. Lorenzen, B. Holst, and R. Redmer, Phys. Rev. B **82**, 195107 (2010).
[27] J. P. Perdew, K. Burke, and M. Ernzerhof, Phys. Rev. Lett. **77**, 3865 (1996).
[28] M. French and R. Redmer, J. Phys.: Condens. Matter **21**, 375101 (2009).
[29] K. Huber and G. Herzberg, *Molecular Spectra and Molecular Structure* (Van Nostrand, New York, 1979).
[30] M. A. Morales, C. Pierleoni, and D. M. Ceperley, Phys. Rev. E **81**, 021202 (2010).
[31] B. Holst, R. Redmer, V. Gryaznov, V. Fortov, and I. Iosilevskiy, Eur. Phys. J. D **66**, 104 (2012).
[32] J. W. Leachman, R. T. Jacobsen, S. G. Penoncello, and E. W. Lemmon, J. Phys. Chem. Ref. Data **38**, 721 (2009).
[33] H. Juranek, R. Redmer, and Y. Rosenfeld, J. Chem. Phys. **117**, 1768 (2002).
[34] L. Caillabet, S. Mazevet, and P. Loubeyre, Phys. Rev. B **83**, 094101 (2011).
[35] L. Caillabet, Ph.D. thesis, École Polytechnique, 2011.
[36] M. A. Morales, C. Pierleoni, E. Schwegler, and D. M. Ceperley, Proc. Natl. Acad. Sci. USA **107**, 12799 (2010).
[37] M. P. Desjarlais, Phys. Rev. B **68**, 064204 (2003).
[38] M. D. Knudson, M. P. Desjarlais, R. W. Lemke, T. R. Mattsson, M. French, N. Nettelmann, and R. Redmer, Phys. Rev. Lett. **108**, 091102 (2012).
[39] W. J. Nellis, M. Ross, and N. Holmes, Science **269**, 1249 (1995).
[40] N. C. Holmes, M. Ross, and W. J. Nellis, Phys. Rev. B **52**, 15835 (1995).
[41] D. Saumon, G. Chabrier, and H. M. van Horn, Astrophys. J. Suppl. Ser. **99**, 713 (1995).

[42]M. French, A. Becker, W. Lorenzen, N. Nettelmann, M. Bethkenhagen, J. Wicht, and R. Redmer, Astrophys. J., Suppl. Ser. **202**, 5 (2012).
[43]V. Kopyshev and V. Khrustalev, J. Appl. Mech. Tech. Phys. **21**, 113 (1980).
[44]V. E. Fortov, V. Y. Ternovoi, M. V. Zhernokletov, M. A. Mochalov, A. L. Mikhailov, A. S. Filimonov, A. A. Pyalling, V. B. Mintsev, V. K. Gryaznov, and I. L. Iosilevskiy, J. Exp. Theor. Phys. **97**, 259 (2003).
[45]P. Loubeyre, R. LeToullec, D. Hausermann, M. Hanfland, R. J. Hemley, H. K. Mao, and L. W. Finger, Nature (London) **383**, 702 (1996).
[46]R. G. Greene, H. Luo, and A. L. Ruoff, Phys. Rev. Lett. **73**, 2075 (1994).
[47]M. A. Morales, J. M. McMahon, C. Pierleoni, and D. M. Ceperley, Phys. Rev. Lett. **110**, 065702 (2013).
[48]A. Chentsov and P. Levashov, Contrib. Plasma Phys. **52**, 33 (2012).
[49]J. Fortney, M. Marley, and J. Barnes, Astrophys. J. **659**, 1661 (2007).